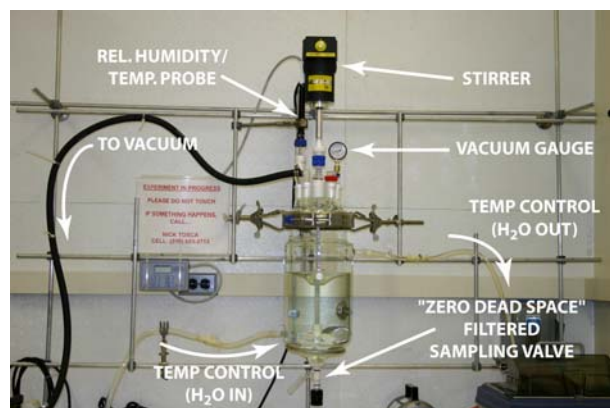


**EXPERIMENTAL CONSTRAINTS ON EVAPORATION PROCESSES AT MERIDIANI PLANUM.** N. J. Tosca<sup>1</sup> and S. M. McLennan<sup>1</sup>, <sup>1</sup>Department of Geosciences, State University of New York, Stony Brook, NY 11794-2100 (ntosca@ic.sunysb.edu).

**Introduction:** In-depth analysis of evaporitic sediments at Meridiani Planum by the *Opportunity* Rover has highlighted the importance of fluid evaporation at the martian surface [1]. Previous work aimed at understanding the controls on evaporation and the resulting mineral assemblages has been largely theoretical [2]. Some recent experimental work has focused on evaporite minerals at the martian surface but has described only the resulting bulk mineralogy produced from fluid evaporation [3,4]. In order to more adequately understand the controls on saline mineral formation and resulting brine compositions, it is imperative that both solution and solid be characterized during the evaporation process itself. Here, we report on the experimental evaporation of synthetic basaltic weathering derived fluids. Complete solution and solid analyses throughout the evaporation process provide a wealth of data that are critical for: (1) understanding kinetic controls and complications that may be present in such geochemical systems and (2) updating and improving future theoretical modeling efforts to provide a more realistic interpretation of the processes involved in saline mineral production at the martian surface [5].

**Methods and Analyses:** The goal of the experiments is to fully characterize chemical changes in the evaporating fluid as well as precipitates produced over the course of the experiment. This is accomplished using the apparatus shown in Fig. 1, which consists of a 5L jacketed borosilicate reaction vessel. The entire vessel is vacuum-sealed via a 5-neck lid. A vacuum is maintained on the apparatus at a



**Figure 1.** Experimental apparatus used in this study.

pressure of approximately 30 mbar. Temperature was maintained at 25°C by circulating water through the jacket from a temperature-controlled water bath. The solution was continuously stirred with a vacuum-sealed PTFE stirrer and temperature as well as relative humidity of the vessel headspace were monitored continuously. At regular intervals,

the solution was sampled through a 50 µm filtered, zero-dead space valve at the bottom of the apparatus. Solutions were filtered again before dilution and analysis with 0.22 µm syringe filters. Solid precipitates were collected 3 days after evaporation to dryness was achieved, to establish equilibrium between solids and the ambient relative humidity in the reaction vessel.

Each solution was analyzed for temperature, Eh and pH. Eh was measured with a platinum electrode and calibrated against ZoBell's solution. Major cations (Na, Mg, Al, K, Ca, Fe) were measured using a DCP atomic emission spectrophotometer. Fe<sup>2+</sup>, Fe<sub>Total</sub>, SO<sub>4</sub> and Cl were measured using a Hach DR/2000 spectrophotometer.

Residual solids were extracted and immediately stored at 25°C in two relative humidity buffered chambers: LiCl (11.3% RH) and KCl (84.34% RH). Solids were analyzed by powder X-ray diffraction (XRD) mounted in silicone grease and by SEM with semi-quantitative EDS analysis to assist in phase identification. XRD results were matched against the Powder Diffraction File 2 database using Crystallographica Search-Match software, allowing for multi-phase analysis.

**Results:** The starting composition of the dilute fluid being evaporated was based on weathering experiments conducted with synthetic olivine-bearing basalt at ~pH 2 [3]. The extent of Fe oxidation (expressed by Fe<sup>2+</sup>/Fe<sub>Total</sub>) was set at approximately 0.48 at the beginning of the experiment to investigate Fe redox disequilibrium during the evaporation process [2]. Because the apparatus is too large to monitor weight loss from evaporation, water loss was determined using mass balance calculations from the most conservative elements (Na and Mg) in solution to arrive at average water loss values for each analysis.

The behavior of all major components in solution is depicted in Figure 2 as a function of water remaining per kg of solvent. There are several instances of fractionation among components in solution during evaporation. The slope derived from the conservative elements provides a reference slope of solution concentration versus water removal. Upon comparison to this slope, the point of precipitation of some minerals can be readily identified. For example, Figure 2 (point A) indicates that gypsum precipitates when approximately 140 g H<sub>2</sub>O / kg remain. At the same point in evaporation, Cl concentration in solution decreases markedly (point B), indicating that the precipitation of gypsum has incorporated a small amount of Cl in the mineral structure or on the surface of the mineral. SEM-EDS analyses on gypsum crystals confirm the presence of Cl.

More detailed analysis of Fe<sup>2+</sup> and Fe<sup>3+</sup> behavior in solution show three indications of Fe fractionation. The first

indication occurs at the beginning of the experiment where  $\text{Fe}^{2+}$  is fractionated relative to  $\text{Fe}^{3+}$  (approx. 500 g  $\text{H}_2\text{O}$  / kg) (Fig. 2, point C). This and other solution data from the initial portion (equilibration of the synthetic fluid) of the experiment suggest that  $\text{Fe}^{3+}$  concentrations may have been briefly controlled by a poorly crystalline precipitate before

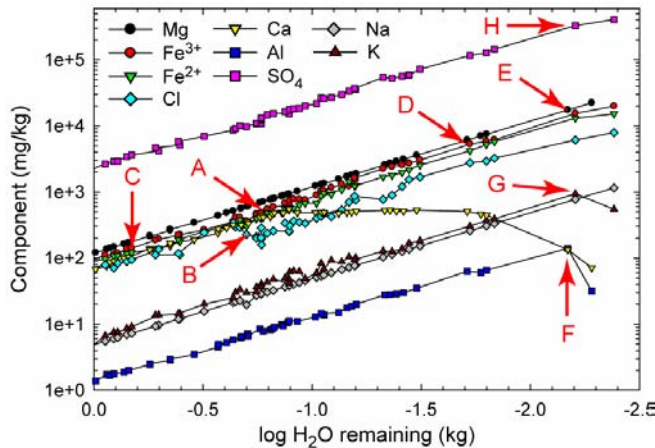


**Figure 2.** Major components in solution and points of solute fractionation during evaporation

evaporation proceeded and the phase was re-dissolved. The second fractionation occurs at approximately 20 g  $\text{H}_2\text{O}$  / kg, where  $\text{Fe}^{3+}$  decreases relative to  $\text{Fe}^{2+}$  (Fig. 2, point D). The third fractionation occurs between the last two data points at approximately 6 g  $\text{H}_2\text{O}$  / kg where both  $\text{Fe}^{2+}$  and  $\text{Fe}^{3+}$  decrease, where  $\text{Fe}^{2+}$  decreases to a greater extent than  $\text{Fe}^{3+}$  (Fig. 2, point E). In addition, between the last two data points, there is a fractionation in Al, K and  $\text{SO}_4$  (Fig. 2, points F-H), all suggesting precipitation of one or more phases at this point in evaporation.

It is important to note that the amount of solution after the last data point was taken was not abundant enough to sample, and further solution concentration beyond this point could not be recorded. In future experiments, late stage brines will be re-created to monitor solution fractionation and mineral precipitation at highly concentrated levels.

Solid analyses from XRD and SEM correspond with solute fractionation observed in the experiment. Major phases that were identified in XRD data were: anhydrite, gypsum, kieserite, szomolnokite and bilinite. SEM analysis confirmed the presence of anhydrite, gypsum, kieserite, and szomolnokite with EDS yielding atomic ratios from analyses on flat, smooth grains. Several of these phases represent the de-hydrated forms of gypsum, epsomite and melanterite, respectively, which were likely the initial phases precipitated from solution owing to lower solubility than their de-hydrated counterparts. The dehydration was likely in response to the ambient relative humidity in the vessel after complete desiccation for 3 days.

In addition, two other distinct Fe and  $\text{SO}_4$ -bearing minerals were found in SEM analyses. One mineral contains

Fe, S and O and has Fe to S ratios that are best matched by bilinite. Also, a K, Fe, S and O-bearing phase was identified which best matches atomic ratios of voltaite, a mixed-valence K-bearing Fe-sulfate. K-jarosite could be easily ruled out because of anomalously low K to S and Fe to S ratios in EDS analyses. Therefore, coupling solution and solid analyses from this experiment, we can confirm the precipitation of gypsum, epsomite, melanterite, bilinite and voltaite from solution and/or solid analyses.

**Discussion and Conclusions:** The results presented here are part of a larger effort to understand the controls imposed on evaporite mineral assemblages at the martian surface by initial solution composition. The experiment described above reproduces a geochemical system relevant to the formation of Meridiani Planum sediments, as suggested by [2]. The results clearly show the complex behavior of Fe as an evaporitic component in evaporative systems evolving from basaltic weathering. In addition, some constraints can be placed on the nature of evaporite mineral formation at Meridiani Planum. For example, jarosite was not found in the saline mineral assemblage formed in this experiment. However, jarosite precipitation is indeed favored during initial solution equilibration at the outset of evaporation. At Meridiani Planum, it is possible that jarosite formed partly as a weathering product before evaporation commenced and was incorporated with siliclastic residue produced from the chemical weathering of basalt. However, the experiments show that by mass, Fe-sulfates are critically important and unless all of the Fe was oxidized before evaporation, some Fe must have participated in the formation of Fe-sulfates similar to those identified in this study. Another equally plausible pathway of jarosite and/or hematite formation at Meridiani Planum is the oxidation of Fe-bearing sulfate minerals such as melanterite, szomolnokite, bilinite and voltaite to produce jarosite, hematite, or hematite precursors.

In addition to shedding light on formation processes at Meridiani Planum, the experimental results represent one particular geochemical environment identified at the martian surface. Future experiments conducted in a "chemical divide" framework will provide critical data on the geochemical processes responsible for producing saline minerals at the martian surface [5]. Such data are also invaluable for the theoretical modeling of such unique geochemical systems and the interpretation of evaporite mineral assemblages at the martian surface [6].

**References:** [1] Squyres, S. & Knoll, A. (2005) *EPSL*, 240, 1. [2] Tosca, N.J. et al. (2005) *EPSL*, 240, 122. [3] Tosca, N.J. et al. (2004) *JGR*, 109, E05003. [4] Golden, D.C. et al. (2005) *JGR*, 110, E12S07. [5] Tosca, N.J. & McLennan, S.M. (2006) *EPSL*, 241, 21. [6] Tosca, N.J. & McLennan, S.M. (2006) *LPS XXXVII, this conference*.